

Controlling the Fluctuating Tip-Enhanced Raman Spectra of Chloramben on Silver Nanocubes

Oliva M. Primera-Pedrozo,^{1,‡} Alexander B. C. Mantilla,^{2,‡} Tanya L. Myers,¹ Yi Gu,² Patrick Z. El-Khoury^{1,*}

¹Physical Sciences Division, Pacific Northwest National Laboratory, P.O. Box 999, Richland, WA 99352, USA

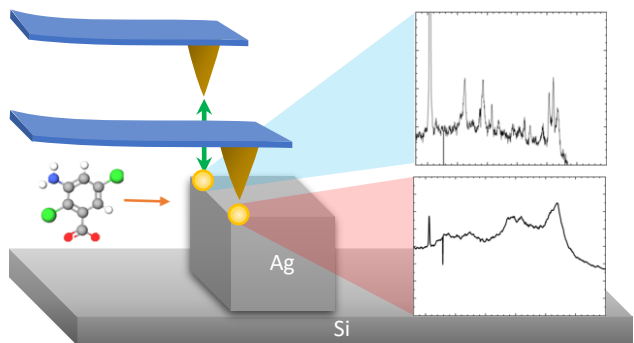
²Department of Physics and Astronomy, Washington State University, Pullman, Washington 99164, USA

[‡]Equal contribution

*Patrick.elkhoury@pnnl.gov

ABSTRACT: Tip-enhanced Raman (TER) scattering from molecules residing at plasmonic junctions can be used to detect, identify, and image single molecules. This is most evident for flat molecules interrogated under extreme conditions of temperatures and pressure. It is also the case for (bio)molecular systems that feature preferred orientations/conformations under ambient laboratory conditions. More complex molecules that can adopt multiple conformations and/or that feature different protonation and/or charge states give rise to complex TER spectra. We illustrate how the latter can be controlled in the case of chloramben molecules coated onto plasmonic silver nanocubes. We show that characteristic molecular Raman spectra cannot be obtained when tunneling plasmons are operative, i.e., when the tip is in direct contact with the chemically functionalized plasmonic nanoparticles. We rationalize these observations and propose an approach to less invasive, and hence, more analytical TER spectral imaging.

TOC



INTRODUCTION

Tip-enhanced Raman (TER) spectral imaging is a powerful approach to chemical and chemical reaction imaging. Its benefits, stemming from the combination of scanning probe and (non)linear optical spectroscopy,^{1, 2} is perhaps most evident in measurements that take advantage of the stability of ultrahigh vacuum/ultralow temperature setups, where sub-molecular resolution has been demonstrated.³⁻⁵ Even though the information content is blurred as a result of thermal fluctuations and instabilities, performing TER measurements under ambient laboratory conditions is appealing, particularly for applications in catalysis and bioimaging that often require interrogating solid-liquid interfaces.⁶⁻⁸

Ambient TER setups are typically built around an atomic force microscope (AFM).⁹ Within the realm of AFM-TER measurements, most reported experiments are performed using contact mode feedback.¹⁰ In other words, optical signals are recorded when the tip exerts force on the sample, see Figure 1. More modern approaches to TER spectral imaging take advantage of hybrid AFM feedback modes, wherein sample motion is achieved using tapping (or intermittent contact) feedback, and nano-optical signals are recorded when the tip is in contact with the sample.¹¹ This mode preserves sample integrity and prolongs the lifetime of the plasmonic probe, all while retaining optimal optical enhancement.

Besides considerations that have to do with mechanical and first order electrostatic interactions between the tip and the sample, there are additional motivations for avoiding the use of contact mode or even hybrid tapping/contact mode feedback in TER spectral imaging.^{11, 12} This is particularly the case for substrates consisting of either extended or nanostructured plasmonic metals, where optimal enhancement and spatial resolution have been demonstrated. Indeed, the interplay between classical and quantum plasmons in plasmonic nano-gaps¹³ complicates the information content in TER, as discussed in recent reports

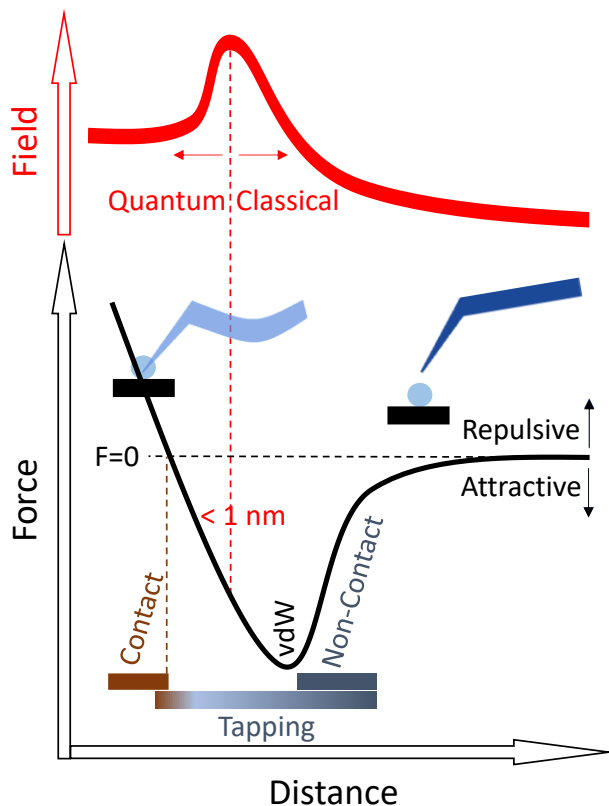


Figure 1. Schematic illustration of a typical AFM force-distance curve (lower black trace) and the expected local optical field enhancement as a function of tip-sample distance (upper red curve). The two curves are annotated to highlight the zero-force line ($F=0$), van der Waals (vdW) contact, (non)contact and tapping mode regimes, and approximate position of the transition from classical to quantum plasmons. Note that the circular blue dot between the tip and sample in the inset designates molecules (e.g., water) that lead to contact and that offset vdW and conductive (< 1 nm) contact points.

from our group.¹² In our recent study, through TER mapping experiments performed either using tapping mode or contact mode feedback, we showed how molecular charging and optical rectification that are noticeable in the latter can be suppressed when tip-sample interactions are minimized.¹² This was associated with localized *vs* quantum plasmon driven TER using tapping *vs* contact mode feedback, as schematically illustrated in Figure 1. Note that as TER signal magnitudes are not just sensitive to local fields but also to molecular scattering cross-sections, the field picture is modified when molecular loads are taken into account. The most mundane consideration in this context is Raman scattering from neutral *vs* anionic species in the two plasmonic regimes depicted in the upper panel of Figure 1, where distinct molecular resonances may be operative.¹⁴

In this study, we initially set out to detect trace quantities of an herbicide, chloramben, *via* TER spectroscopy and imaging. The detection of herbicide residues (as well as pesticide residues and other metabolites) has traditionally involved the use of chromatography-mass spectrometry¹⁵ and high-performance liquid chromatography.¹⁶ Near-field spectroscopy draws interest as a plausible alternative.

Besides general interest in the ultrasensitive detection and identification of pesticides and herbicides,¹⁷⁻²¹ chloramben features an interesting chemical structure from fundamental and applied surface science/spectroscopy perspectives, see Figure 2. Namely, this molecule has two possibilities of binding onto a plasmonic metal, herein a silver nanocube. The first possibility is binding through the NH₂ moiety and the second involves the CO₂H group. These structural and binding motifs are common to many small biomolecules, including amino acids. Besides distinct binding geometries, different protonation and charge states are also possible for silver bound chloramben molecules under ambient laboratory conditions. Modified TER surface selection rules, the possibility of multipolar TER scattering, and optical rectification add further complexity to the recorded spectral patterns.¹¹ In the following, we show how all these effects together lead to extreme spectral heterogeneity: the molecule is not recognizable from our recorded contact mode TER spectra.

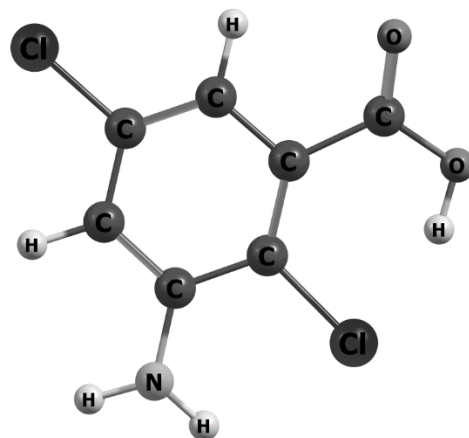


Figure 2. Molecular structure of chloramben (3-Amino-2,5-dichlorobenzoic acid).

RESULTS AND DISCUSSION

Simultaneously recorded AFM and TER maps of the edge of a chloramben-coated silver nanocube are shown in Figure 3. These images were recorded using a hybrid feedback mode: sample motion is accomplished using tapping mode feedback, whereas TER spectra are recorded when the tip is in contact with the substrate, i.e., above the zero force ($F=0$) line in Figure 1. The AFM (Figure 3a) and TER (Figure 3b) images are both indicative of a complex tip morphology. Indeed, deviations from the expected field profile can be associated with artifacts both in AFM as well as TER imaging.²² The more important observation is the extreme spectral heterogeneity across the

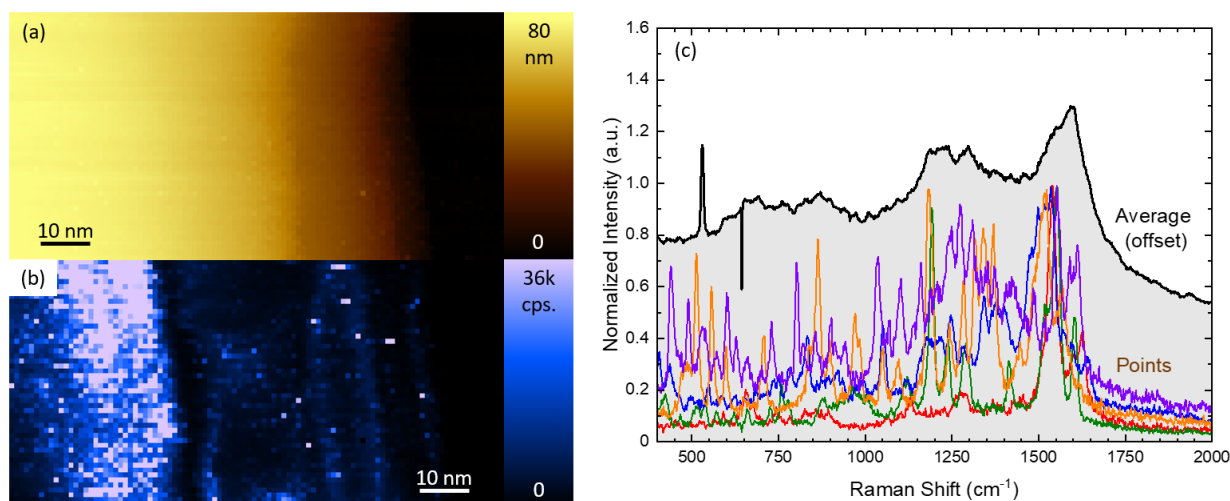


Figure 3. Simultaneously recorded AFM (a) and contact mode TER (b, binned in the 1500-1700 cm^{-1} spectral region) images of the edge of a chloramben-coated plasmonic silver nanocube. Selected single pixel TER spectra are shown in (c) along with the optical response that we obtained by spatial averaging over the entire area in (b). Parameters: 100 $\mu\text{W}/\mu\text{m}^2$ at the sample position, 1 nm lateral/vertical steps, 0.25 s/pixel time integration.

map, which can be seen in Figure 3c. The recorded single pixel spectra are highly congested, consisting of numerous sharp molecular lines that span the entire 500-1700 cm^{-1} spectral region. Note that these observations (Figure 3c) are quite general: extreme spectral heterogeneity was observed in the TER spectral images of various chloramben-coated surfaces and nanostructures, see Figure S1. In other words, these observations are not a function of any specific tip geometry or nanoparticle shape/makeup. None of the spectra we recorded can be reliably used to identify the chloramben molecules that we deposited onto the nanocube. It is interesting to stress that this is not the case for aromatic thiol derivatives interrogated under nearly identical conditions.¹¹ If one assumes that the operative local optical fields are similar in this study *vs* prior work irrespective of the molecular load, the observation of extreme spectral heterogeneity must have to do with our current choice of molecule. So, beyond the realm of functionalized aromatic thiols, a few dye molecules, and porphyrins immobilized in UHV chambers, how can one use TER as a non-invasive analytical chemical imaging and identification technique without having to over-engineer the sample or tip?

Before attempting to offer one answer to the question raised above, we consider the spatio-temporally averaged TER response in Figure 3c. This response is similar to traces often seen in diffraction-limited surface enhanced Raman scattering measurements. There, similar spectra are often associated with amorphous carbon that forms as a result of sample (photo)damage.^{23, 24} In other instances, observations of broad and featureless spectra are assigned to flat binding orientations,²⁵ a classic example of which is enhanced Raman scattering from benzene molecules physisorbed onto plasmonic metals.²⁶ Our present results clearly establish that extreme spectral heterogeneity can also lead to broadened background-like spectral profiles upon spatial and temporal averaging. This effect is often under-appreciated in the plasmon-enhanced (surface-enhanced in particular) Raman community but should be considered. In the same vein, the analysis

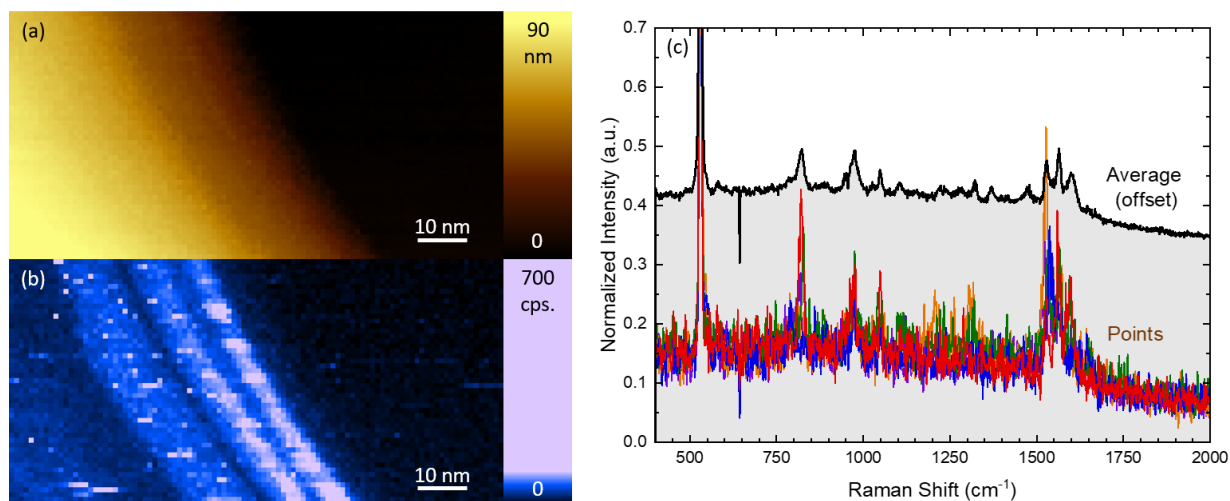


Figure 4. Simultaneously recorded AFM (a) and tapping mode TER (b, binned in the 1500-1700 cm^{-1} spectral region) images of the edge of a chloramben-coated plasmonic silver nanocube. Selected single pixel TER spectra are shown in (c) along with the optical response that we obtained by spatial averaging over the entire area in (b). Parameters: $100 \mu\text{W}/\mu\text{m}^2$ at the sample position, 1 nm lateral/vertical steps, 0.5 s/pixel time integration.

of surface-enhanced and TER backgrounds must also account for molecular processes that lead to broad background-like features.

Inspired by recent observations¹² that were highlighted in the introductory comments, we repeated the measurements above using the same tip and nanoparticle, but now using tapping mode feedback, see Figure 4. The stark contrast between the well-defined spectra in Figure 4c and the disparate spectra in Figure 3c is immediately evident. The spectra we observe in Figure 4c can be assigned to chloramben on the basis of standard gas phase density functional theory simulations (see Figure S2). The high spatial resolution observed in Figure 4b (~ 2 nm) suggests that this approach may be used to readily detect and to identify yoctomolar concentrations of chloramben molecules under ambient laboratory conditions. The sample preparation that consists of simply drop-casting solvated chloramben onto a substrate is an added advantage.

A side-to-side comparison between the tapping mode (Figure 4) and contact mode (Figure 3) spectra allows us to draw a few key conclusions. Molecular aspects alone, such as the possibility of multiple orientations/conformations, cannot explain the observed spectral heterogeneity in contact mode vs uniform spectral patterns in tapping mode TER spectral imaging. The same can be said of mechanical deformations, i.e., molecular flattening when the tip exerts force on the silver-bound molecules. Namely, what we observe are sharp molecular lines that undergo extreme spectral diffusion. A plausible explanation for our observations requires invoking the distinct (non)local fields that drive the optical processes in tapping vs contact mode measurements. As schematically illustrated in Figure 1 and discussed in prior reports,¹² tunneling plasmons drive TER when conductive contact is established between the probe and the surface. The onset of tunneling is accompanied by optical rectification and molecular charging. Whereas the first is not expected to significantly alter the spectra barring Stark reporters (e.g., nitrile moieties),²⁷ the second can have more significant effects on the observables. For instance, the possibility of

resonance enhancement upon molecular charging has been recently invoked in the context of plasmon-enhanced Raman scattering.¹⁴ Similarly, we herein propose that molecular charging shifts molecular resonances into the spectral window that we access with our excitation wavelength. We propose that this is at the core of the observed spectral variations. Distinct conformations/orientations/binding motifs that may alter the static/dynamic polarizabilities of silver-bound molecules also contribute to our observation of extreme spectral diffusion in contact mode TER experiments. The suppression of molecular charging in tapping mode TER measurements on the other hand leads to recognizable and assignable molecular line spectra that can be understood on the basis of simple simulations, as shown in Figure S2.

CONCLUSIONS

In conclusion, tapping mode TER spectral imaging is the recommended approach for the detection and identification of molecules that do not adopt well-defined binding geometries or conformations. Recent observations of brighter signals in tapping mode *vs* contact mode TER experiments²⁸ provide additional motivation for adopting the former in Raman nanoscopy. A study that described how to optimize signal levels in tapping mode nano-optical measurements¹⁰ is equally important in this context. Alternatively, it would be attractive to develop modified contact mode feedback methods, wherein the force exerted on the sample is below the zero force line. Here, the objective would be to maintain 1-2 nm separation between the tip and substrate throughout the measurements using (negative or attractive) force for feedback. Novel scalable approaches to functionalizing metal tips and substrates with ultrathin (1-2 nm) insulator layers continue to be employed in UHV-TER systems. It would be interesting to explore the same tactic for measurements performed under ambient laboratory conditions.

SUPPORTING INFORMATION

Experimental details, additional TER spectra recorded using different tips and plasmonic constructs, and a comparison between computed gas phase density functional theory and experimental Raman spectra

The supporting information is available free of charge at pubs.acs.org

AUTHOR INFORMATION

Corresponding Author

Patrick Z. El-Khoury –*Physical Sciences Division, Pacific Northwest National Laboratory, Richland, Washington 99352, United States; orcid.org/0000-0002-6032-9006*
Email: patrick.elkhoury@pnnl.gov

Authors

Oliva M. Primera-Pedrozo—*Physical Sciences Division, Pacific Northwest National Laboratory, Richland, Washington 99352, United States; orcid.org/0000-0002-6109-2020*

Alexander B. C. Mantilla—*Department of Physics and Astronomy, Washington State University, Pullman, Washington 99164, United States; orcid.org/0000-0002-9262-1351*

Tanya L. Myers—*Physical Sciences Division, Pacific Northwest National Laboratory, Richland, Washington 99352, United States; orcid.org/0000-0001-8995-7033*

Yi Gu—*Department of Physics and Astronomy, Washington State University, Pullman, Washington 99164, United States*

ACKNOWLEDGMENTS

A.B.C.M. and Y.G. acknowledge support from the National Science Foundation (DMR-2004655). P.Z.E and O.M.P.P acknowledge support from the U.S. Department of Energy, Office of Science, Basic Energy Sciences, Chemical Sciences, Geosciences, and Biosciences Division, Condensed Phase and Interfacial Molecular Science program, FWP 16248.

Competing Interest Statement. YG has equity interest in Klar Scientific.

REFERENCES

- (1) Stöckle, R. M.; Suh, Y. D.; Deckert, V.; Zenobi, R. Nanoscale chemical analysis by tip-enhanced Raman spectroscopy. *Chem. Phys. Lett.* **2000**, *318* (1), 131-136.
- (2) Kurouski, D.; Dazzi, A.; Zenobi, R.; Centrone, A. Infrared and Raman chemical imaging and spectroscopy at the nanoscale. *Chem. Soc. Rev.* **2020**, *49* (11), 3315-3347.
- (3) Zhang, R.; Zhang, Y.; Dong, Z. C.; Jiang, S.; Zhang, C.; Chen, L. G.; Zhang, L.; Liao, Y.; Aizpurua, J.; Luo, Y.; Yang, J. L.; Hou, J. G. Chemical mapping of a single molecule by plasmon-enhanced Raman scattering. *Nature* **2013**, *498* (7452), 82-86.
- (4) Lee, J.; Crampton, K. T.; Tallarida, N.; Apkarian, V. A. Visualizing vibrational normal modes of a single molecule with atomically confined light. *Nature* **2019**, *568* (7750), 78-82.
- (5) Schultz, J. F.; Mahapatra, S.; Li, L.; Jiang, N. The Expanding Frontiers of Tip-Enhanced Raman Spectroscopy. *Appl. Spectrosc.* **2020**, *74* (11), 1313-1340.
- (6) Britz-Grell, A. B.; Saumer, M.; Tarasov, A. Challenges and Opportunities of Tip-Enhanced Raman Spectroscopy in Liquids. *J. Phys. Chem. C* **2021**, *125* (39), 21321-21340.
- (7) Wang, Y.-Z.; Wang, J.; Wang, X.; Ren, B. Electrochemical tip-enhanced Raman spectroscopy for in situ study of electrochemical systems at nanoscale. *Curr. Opin. Electrochem.* **2023**, *42*, 101385.
- (8) Wang, X.; Huang, S.-C.; Huang, T.-X.; Su, H.-S.; Zhong, J.-H.; Zeng, Z.-C.; Li, M.-H.; Ren, B. Tip-enhanced Raman spectroscopy for surfaces and interfaces. *Chem. Soc. Rev.* **2017**, *46* (13), 4020-4041.
- (9) Verma, P. Tip-Enhanced Raman Spectroscopy: Technique and Recent Advances. *Chem. Rev.* **2017**, *117* (9), 6447-6466.
- (10) Umakoshi, T.; Kawashima, K.; Moriyama, T.; Kato, R.; Verma, P. Tip-enhanced Raman spectroscopy with amplitude-controlled tapping-mode AFM. *Sci. Rep.* **2022**, *12* (1), 12776.
- (11) El-Khoury, P. Z. Tip-Enhanced Raman Scattering on Both Sides of the Schrödinger Equation. *Acc. Chem. Res.* **2021**, *54* (24), 4576-4583.
- (12) Wang, C.-F.; O'Callahan, B. T.; Kurouski, D.; Krayev, A.; Schultz, Z. D.; El-Khoury, P. Z. Suppressing Molecular Charging, Nanochemistry, and Optical Rectification in the Tip-Enhanced Raman Geometry. *J. Phys. Chem. Lett.* **2020**, *11* (15), 5890-5895.
- (13) Zhu, W.; Esteban, R.; Borisov, A. G.; Baumberg, J. J.; Nordlander, P.; Lezec, H. J.; Aizpurua, J.; Crozier, K. B. Quantum mechanical effects in plasmonic structures with subnanometre gaps. *Nat. Commun.* **2016**, *7* (1), 11495.
- (14) Sloan-Dennison, S.; Zoltowski, C. M.; El-Khoury, P. Z.; Schultz, Z. D. Surface Enhanced Raman Scattering Selectivity in Proteins Arises from Electron Capture and Resonant Enhancement of Radical Species. *J. Phys. Chem. C* **2020**, *124* (17), 9548-9558.
- (15) Alder, L.; Greulich, K.; Kempe, G.; Vieth, B. Residue analysis of 500 high priority pesticides: Better by GC-MS or LC-MS/MS? *Mass Spectrom. Rev.* **2006**, *25* (6), 838-865.
- (16) Michel, M.; Buszewski, B. HPLC DETERMINATION OF PESTICIDE RESIDUE ISOLATED FROM FOOD MATRICES. *J. Liq. Chromatogr. Relat. Technol.* **2002**, *25* (13-15), 2293-2306.
- (17) Dong, X.; Tang, Z.; Zhang, H.; Hu, Y.; Yao, Z.; Huang, R.; Bai, J.; Yang, Y.; Hong, W. Ultrasensitive Detection of Organophosphorus Pesticides Using Single-Molecule Conductance Measurement. *Anal. Chem.* **2023**, *95* (26), 9831-9838.
- (18) Li, B.; Wang, Z. Ultrasensitive Pesticide Detection and Specific Recognition in Microenvironment-Modulated Fluorescent Micro-/Mesoporous Polyaminals. *ACS Appl. Mater. Interfaces* **2023**, *15* (26), 31824-31835.
- (19) Sheng, E.; Lu, Y.; Xiao, Y.; Li, Z.; Wang, H.; Dai, Z. Simultaneous and ultrasensitive detection of three pesticides using a surface-enhanced Raman scattering-based lateral flow assay test strip. *Biosens. Bioelectron.* **2021**, *181*, 113149.

- (20) Lee, D. K.; Kim, G.; Kim, C.; Jhon, Y. M.; Kim, J. H.; Lee, T.; Son, J. H.; Seo, M. Ultrasensitive Detection of Residual Pesticides Using THz Near-Field Enhancement. *IEEE Trans. Terahertz Sci. Technol.* **2016**, *6* (3), 389-395.
- (21) Ashrafi Tafreshi, F.; Fatahi, Z.; Ghasemi, S. F.; Taherian, A.; Esfandiari, N. Ultrasensitive fluorescent detection of pesticides in real sample by using green carbon dots. *PLOS ONE* **2020**, *15* (3), e0230646.
- (22) Wang, C.-F.; O'Callahan, B. T.; Arey, B. W.; Kurouski, D.; El-Khoury, P. Z. High-Resolution Raman Nano-Imaging with an Imperfect Probe. *J. Phys. Chem. C* **2022**, *126* (8), 4089-4094.
- (23) Heck, C.; Kanehira, Y.; Kneipp, J.; Bald, I. Amorphous Carbon Generation as a Photocatalytic Reaction on DNA-Assembled Gold and Silver Nanostructures. *Molecules* **2019**, *24* (12), 2324.
- (24) Zong, C.; Xu, M.; Xu, L.-J.; Wei, T.; Ma, X.; Zheng, X.-S.; Hu, R.; Ren, B. Surface-Enhanced Raman Spectroscopy for Bioanalysis: Reliability and Challenges. *Chem. Rev.* **2018**, *118* (10), 4946-4980.
- (25) El-Khoury, P. Z.; Peppernick, S. J.; Hu, D.; Joly, A. G.; Hess, W. P. The Origin of Surface-Enhanced Raman Scattering of 4,4'-Biphenyldicarboxylate on Silver Substrates. *J. Phys. Chem. C* **2013**, *117* (14), 7260-7268.
- (26) Gao, X.; Davies, J. P.; Weaver, M. J. Test of surface selection rules for surface-enhanced Raman scattering: the orientation of adsorbed benzene and monosubstituted benzenes on gold. *J. Phys. Chem.* **1990**, *94* (17), 6858-6864.
- (27) Wang, H.; Yao, K.; Parkhill, J. A.; Schultz, Z. D. Detection of electron tunneling across plasmonic nanoparticle-film junctions using nitrile vibrations. *Phys. Chem. Chem. Phys.* **2017**, *19* (8), 5786-5796.
- (28) Bartolomeo, G. L.; Zhang, Y.; Kumar, N.; Zenobi, R. Molecular Perturbation Effects in AFM-Based Tip-Enhanced Raman Spectroscopy: Contact versus Tapping Mode. *Anal. Chem.* **2021**, *93* (46), 15358-15364.